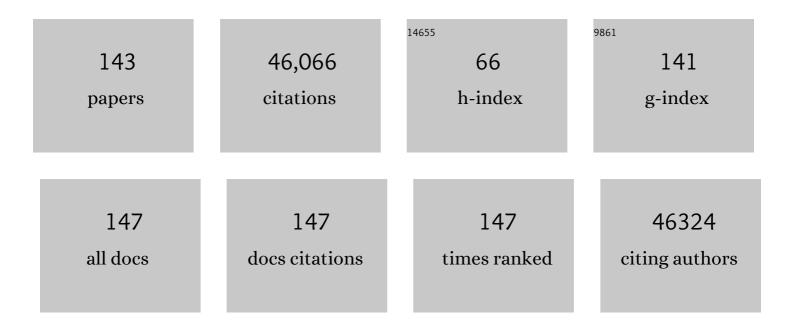
List of Publications by Year in descending order

Source: https://exaly.com/author-pdf/3149914/publications.pdf Version: 2024-02-01



COVI EDA

| # | Article | IF | CITATIONS |
|----|---|------|-----------|
| 1 | The chemistry of two-dimensional layered transition metal dichalcogenide nanosheets. Nature Chemistry, 2013, 5, 263-275. | 13.6 | 8,051 |
| 2 | Large-area ultrathin films of reduced graphene oxide as a transparent and flexible electronic material. Nature Nanotechnology, 2008, 3, 270-274. | 31.5 | 4,057 |
| 3 | Photoluminescence from Chemically Exfoliated MoS ₂ . Nano Letters, 2011, 11, 5111-5116. | 9.1 | 3,402 |
| 4 | Graphene oxide as a chemically tunable platform for optical applications. Nature Chemistry, 2010, 2, 1015-1024. | 13.6 | 2,966 |
| 5 | Enhanced catalytic activity in strained chemically exfoliated WS2 nanosheets for hydrogen evolution. Nature Materials, 2013, 12, 850-855. | 27.5 | 2,326 |
| 6 | Chemically Derived Graphene Oxide: Towards Largeâ€Area Thinâ€Film Electronics and Optoelectronics. Advanced Materials, 2010, 22, 2392-2415. | 21.0 | 2,018 |
| 7 | Conducting MoS ₂ Nanosheets as Catalysts for Hydrogen Evolution Reaction. Nano Letters, 2013, 13, 6222-6227. | 9.1 | 1,948 |
| 8 | Blue Photoluminescence from Chemically Derived Graphene Oxide. Advanced Materials, 2010, 22, 505-509. | 21.0 | 1,824 |
| 9 | Evolution of Electronic Structure in Atomically Thin Sheets of WS ₂ and WSe ₂ . ACS Nano, 2013, 7, 791-797. | 14.6 | 1,690 |
| 10 | Evolution of Electrical, Chemical, and Structural Properties of Transparent and Conducting Chemically Derived Graphene Thin Films. Advanced Functional Materials, 2009, 19, 2577-2583. | 14.9 | 1,603 |
| 11 | Atomic and Electronic Structure of Graphene-Oxide. Nano Letters, 2009, 9, 1058-1063. | 9.1 | 1,043 |
| 12 | Coherent Atomic and Electronic Heterostructures of Single-Layer MoS ₂ . ACS Nano, 2012, 6, 7311-7317. | 14.6 | 806 |
| 13 | Lattice dynamics in mono- and few-layer sheets of WS2 and WSe2. Nanoscale, 2013, 5, 9677. | 5.6 | 724 |
| 14 | Graphene-based Composite Thin Films for Electronics. Nano Letters, 2009, 9, 814-818. | 9.1 | 639 |
| 15 | Tunable Photoluminescence from Graphene Oxide. Angewandte Chemie - International Edition, 2012, 51, 6662-6666. | 13.8 | 584 |
| 16 | Insulator to Semimetal Transition in Graphene Oxide. Journal of Physical Chemistry C, 2009, 113, 15768-15771. | 3.1 | 577 |
| 17 | Origin of Indirect Optical Transitions in Few-Layer MoS ₂ , WS ₂ , and WSe ₂ . Nano Letters, 2013, 13, 5627-5634. | 9.1 | 435 |
| 18 | Electronic Properties of Graphene Encapsulated with Different Two-Dimensional Atomic Crystals. Nano Letters, 2014, 14, 3270-3276. | 9.1 | 433 |

| # | Article | IF | CITATIONS |
|----|---|---------------------------------------|------------|
| 19 | Transport Properties of Monolayer MoS ₂ Grown by Chemical Vapor Deposition. Nano Letters, 2014, 14, 1909-1913. | 9.1 | 431 |
| 20 | Two-Dimensional Crystals: Managing Light for Optoelectronics. ACS Nano, 2013, 7, 5660-5665. | 14.6 | 398 |
| 21 | Controlling many-body states by the electric-field effect in a two-dimensional material. Nature, 2016, 529, 185-189. | 27.8 | 385 |
| 22 | Photocarrier relaxation pathway in two-dimensional semiconducting transition metal dichalcogenides. Nature Communications, 2014, 5, 4543. | 12.8 | 372 |
| 23 | Halide-assisted atmospheric pressure growth of large WSe2 and WS2 monolayer crystals. Applied Materials Today, 2015, 1, 60-66. | 4.3 | 372 |
| 24 | Transparent and conducting electrodes for organic electronics from reduced graphene oxide. Applied Physics Letters, 2008, 92, . | 3.3 | 368 |
| 25 | Electronic transport properties of transition metal dichalcogenide field-effect devices: surface and interface effects. Chemical Society Reviews, 2015, 44, 7715-7736. | 38.1 | 353 |
| 26 | Molecularly thin two-dimensional hybrid perovskites with tunable optoelectronic properties due to reversible surface relaxation. Nature Materials, 2018, 17, 908-914. | 27.5 | 295 |
| 27 | Vapour–liquid–solid growth of monolayer MoS2 nanoribbons. Nature Materials, 2018, 17, 535-542. | 27.5 | 286 |
| 28 | Graphene and Mobile Ions: The Key to All-Plastic, Solution-Processed Light-Emitting Devices. ACS Nano, 2010, 4, 637-642. | 14.6 | 266 |
| 29 | Field emission from graphene based composite thin films. Applied Physics Letters, 2008, 93, . | 3.3 | 258 |
| 30 | Giant photoluminescence enhancement in tungsten-diselenide–gold plasmonic hybrid structures. Nature Communications, 2016, 7, 11283. | 12.8 | 244 |
| 31 | Improved conductivity of transparent single-wall carbon nanotube thin films via stable postdeposition functionalization. Applied Physics Letters, 2007, 90, 121913. | 3.3 | 219 |
| 32 | Nonlinear photoluminescence in atomically thin layered <mml:math xmlns:mml="http://www.w3.org/1998/Math/MathML"><mml:msub><mml:mi>WSe</mml:mi><mml:mn>2from diffusion-assisted exciton-exciton annihilation. Physical Review B, 2014, 90, .</mml:mn></mml:msub></mml:math | l:m 8.2 <td>nl:monsub></td> | nl:monsub> |
| 33 | Large Thermoelectricity via Variable Range Hopping in Chemical Vapor Deposition Grown Single-Layer MoS ₂ . Nano Letters, 2014, 14, 2730-2734. | 9.1 | 210 |
| 34 | Highly Uniform 300 mm Wafer-Scale Deposition of Single and Multilayered Chemically Derived Graphene Thin Films. ACS Nano, 2010, 4, 524-528. | 14.6 | 209 |
| 35 | Evidence for Fast Interlayer Energy Transfer in MoSe ₂ /WS ₂ Heterostructures. Nano Letters, 2016, 16, 4087-4093. | 9.1 | 205 |
| 36 | Colossal Ultraviolet Photoresponsivity of Few-Layer Black Phosphorus. ACS Nano, 2015, 9, 8070-8077. | 14.6 | 204 |

| # | Article | IF | CITATIONS |
|----|---|------|-----------|
| 37 | All-electric magnetization switching and Dzyaloshinskii–Moriya interaction in WTe2/ferromagnet heterostructures. Nature Nanotechnology, 2019, 14, 945-949. | 31.5 | 177 |
| 38 | Chemical Stabilization of 1T′ Phase Transition Metal Dichalcogenides with Giant Optical Kerr Nonlinearity. Journal of the American Chemical Society, 2017, 139, 2504-2511. | 13.7 | 171 |
| 39 | Discovery of a new type of topological Weyl fermion semimetal state in MoxW1â^'xTe2. Nature Communications, 2016, 7, 13643. | 12.8 | 163 |
| 40 | Electronic Structure and Optical Signatures of Semiconducting Transition Metal Dichalcogenide Nanosheets. Accounts of Chemical Research, 2015, 48, 91-99. | 15.6 | 149 |
| 41 | Controlling the magnetic anisotropy in Cr2Ge2Te6 by electrostatic gating. Nature Electronics, 2020, 3, 460-465. | 26.0 | 145 |
| 42 | An innovative way of etching MoS2: Characterization and mechanistic investigation. Nano Research, 2013, 6, 200-207. | 10.4 | 140 |
| 43 | Field Emission from Atomically Thin Edges of Reduced Graphene Oxide. ACS Nano, 2011, 5, 4945-4952. | 14.6 | 139 |
| 44 | Photoelectrochemical properties of chemically exfoliated MoS2. Journal of Materials Chemistry A, 2013, 1, 8935. | 10.3 | 137 |
| 45 | Crested two-dimensional transistors. Nature Nanotechnology, 2019, 14, 223-226. | 31.5 | 129 |
| 46 | Reconfiguring crystal and electronic structures of MoS2 by substitutional doping. Nature Communications, 2018, 9, 199. | 12.8 | 128 |
| 47 | Rapid visualization of grain boundaries in monolayer MoS2 by multiphoton microscopy. Nature Communications, 2017, 8, 15714. | 12.8 | 120 |
| 48 | Engineering Bandgaps of Monolayer MoS ₂ and WS ₂ on Fluoropolymer Substrates by Electrostatically Tuned Manyâ€Body Effects. Advanced Materials, 2016, 28, 6457-6464. | 21.0 | 116 |
| 49 | Exciton–Plasmon Coupling and Electromagnetically Induced Transparency in Monolayer Semiconductors Hybridized with Ag Nanoparticles. Advanced Materials, 2016, 28, 2709-2715. | 21.0 | 115 |
| 50 | Bead-to-fiber transition in electrospun polystyrene. Journal of Applied Polymer Science, 2007, 106, 475-487. | 2.6 | 110 |
| 51 | Synergistic additive-mediated CVD growth and chemical modification of 2D materials. Chemical Society Reviews, 2019, 48, 4639-4654. | 38.1 | 108 |
| 52 | Complex electrical permittivity of the monolayer molybdenum disulfide (MoS_2) in near UV and visible. Optical Materials Express, 2015, 5, 447. | 3.0 | 104 |
| 53 | Growth of Nb-Doped Monolayer WS ₂ by Liquid-Phase Precursor Mixing. ACS Nano, 2019, 13, 10768-10775. | 14.6 | 102 |
| 54 | Selectively Plasmon-Enhanced Second-Harmonic Generation from Monolayer Tungsten Diselenide on Flexible Substrates. ACS Nano, 2018, 12, 1859-1867. | 14.6 | 97 |

| # | Article | IF | CITATIONS |
|----|--|------|-----------|
| 55 | Reduced Graphene Oxide Electrodes for Large Area Organic Electronics. Advanced Materials, 2011, 23, 1558-1562. | 21.0 | 92 |
| 56 | Excitonic Properties of Chemically Synthesized 2D Organic–Inorganic Hybrid Perovskite Nanosheets. Advanced Materials, 2018, 30, e1704055. | 21.0 | 92 |
| 57 | Substitutional doping in 2D transition metal dichalcogenides. Nano Research, 2021, 14, 1668-1681. | 10.4 | 92 |
| 58 | Room-temperature nonlinear Hall effect and wireless radiofrequency rectification in Weyl semimetal TalrTe4. Nature Nanotechnology, 2021, 16, 421-425. | 31.5 | 91 |
| 59 | Heterointerface Screening Effects between Organic Monolayers and Monolayer Transition Metal Dichalcogenides. ACS Nano, 2016, 10, 2476-2484. | 14.6 | 87 |
| 60 | Electroluminescent Devices Based on 2D Semiconducting Transition Metal Dichalcogenides. Advanced Materials, 2018, 30, e1802687. | 21.0 | 86 |
| 61 | Incorporation of graphene in quantum dot sensitized solar cells based on ZnO nanorods. Chemical Communications, 2011, 47, 6084. | 4.1 | 82 |
| 62 | Giant gate-tunable bandgap renormalization and excitonic effects in a 2D semiconductor. Science Advances, 2019, 5, eaaw2347. | 10.3 | 80 |
| 63 | Partially oxidized graphene as a precursor to graphene. Journal of Materials Chemistry, 2011, 21, 11217. | 6.7 | 76 |
| 64 | Photoluminescence Upconversion by Defects in Hexagonal Boron Nitride. Nano Letters, 2018, 18, 6898-6905. | 9.1 | 76 |
| 65 | Efficient Carrier-to-Exciton Conversion in Field Emission Tunnel Diodes Based on MIS-Type van der Waals Heterostack. Nano Letters, 2017, 17, 5156-5162. | 9.1 | 71 |
| 66 | Revealing the Atomic Defects of WS ₂ Governing Its Distinct Optical Emissions. Advanced Functional Materials, 2018, 28, 1704210. | 14.9 | 69 |
| 67 | Effect of oxygen and ozone on p-type doping of ultra-thin WSe ₂ and MoSe ₂ field effect transistors. Physical Chemistry Chemical Physics, 2016, 18, 4304-4309. | 2.8 | 68 |
| 68 | van der Waals Force: A Dominant Factor for Reactivity of Graphene. Nano Letters, 2015, 15, 319-325. | 9.1 | 65 |
| 69 | Charge transport in ion-gated mono-, bi- and trilayer MoS2 field effect transistors. Scientific Reports, 2014, 4, 7293. | 3.3 | 64 |
| 70 | Thermal dissociation of inter-layer excitons in MoS ₂ /MoSe ₂ hetero-bilayers. Nanoscale, 2017, 9, 6674-6679. | 5.6 | 64 |
| 71 | Electronic transport in graphene-based heterostructures. Applied Physics Letters, 2014, 104, . | 3.3 | 61 |
| 72 | Direct white light emission from inorganic–organic hybrid semiconductor bulk materials. Journal of Materials Chemistry, 2010, 20, 10676. | 6.7 | 58 |

| # | Article | IF | CITATIONS |
|----|--|------|-----------|
| 73 | Free-standing graphene on microstructured silicon vertices for enhanced field emission properties. Nanoscale, 2012, 4, 3069. | 5.6 | 58 |
| 74 | Solvent effects on jet evolution during electrospinning of semi-dilute polystyrene solutions. European Polymer Journal, 2007, 43, 1154-1167. | 5.4 | 57 |
| 75 | Two-step fabrication of single-layer rectangular SnSe flakes. 2D Materials, 2017, 4, 021026. | 4.4 | 57 |
| 76 | Characterization of the second- and third-harmonic optical susceptibilities of atomically thin tungsten diselenide. Scientific Reports, 2018, 8, 10035. | 3.3 | 57 |
| 77 | Giant second-harmonic generation in ferroelectric NbOI2. Nature Photonics, 2022, 16, 644-650. | 31.4 | 57 |
| 78 | Highly Stable Twoâ€Dimensional Tin(II) Iodide Hybrid Organic–Inorganic Perovskite Based on Stilbene Derivative. Advanced Functional Materials, 2019, 29, 1904810. | 14.9 | 55 |
| 79 | Evidence for line width and carrier screening effects on excitonic valley relaxation in 2D semiconductors. Nature Communications, 2018, 9, 2598. | 12.8 | 52 |
| 80 | Improving carrier mobility in two-dimensional semiconductors with rippled materials. Nature Electronics, 2022, 5, 489-496. | 26.0 | 52 |
| 81 | Bead structure variations during electrospinning of polystyrene. Journal of Materials Science, 2006, 41, 5704-5708. | 3.7 | 51 |
| 82 | Stable Monolayer Transition Metal Dichalcogenide Ordered Alloys with Tunable Electronic Properties. Journal of Physical Chemistry C, 2016, 120, 2501-2508. | 3.1 | 51 |
| 83 | Zinc oxide nanowire networks for macroelectronic devices. Applied Physics Letters, 2009, 94, . | 3.3 | 49 |
| 84 | Optoelectronic Properties of a van der Waals WS ₂ Monolayer/2D Perovskite Vertical Heterostructure. ACS Applied Materials & Interfaces, 2020, 12, 45235-45242. | 8.0 | 49 |
| 85 | Polarized Lightâ€Emitting Diodes Based on Anisotropic Excitons in Fewâ€Layer ReS ₂ . Advanced Materials, 2020, 32, e2001890. | 21.0 | 49 |
| 86 | Determination of Crystal Axes in Semimetallic T′â€MoTe ₂ by Polarized Raman Spectroscopy. Advanced Functional Materials, 2017, 27, 1604799. | 14.9 | 47 |
| 87 | Nonlinear optical properties of a one-dimensional coordination polymer. Journal of Materials Chemistry C, 2017, 5, 2936-2941. | 5.5 | 46 |
| 88 | Graphene oxide gate dielectric for graphene-based monolithic field effect transistors. Applied Physics Letters, 2013, 102, . | 3.3 | 43 |
| 89 | High-Energy Gain Upconversion in Monolayer Tungsten Disulfide Photodetectors. Nano Letters, 2019, 19, 5595-5603. | 9.1 | 41 |
| 90 | Macroporous polymer nanocomposites synthesised from high internal phase emulsion templates stabilised by reduced graphene oxide. Polymer, 2014, 55, 395-402. | 3.8 | 39 |

| # | Article | IF | CITATIONS |
|-----|--|------|-----------|
| 91 | Nonlinear magnetotransport shaped by Fermi surface topology and convexity. Nature Communications, 2019, 10, 1290. | 12.8 | 38 |
| 92 | Dynamic Structural Evolution of Metal–Metal Bonding Network in Monolayer WS ₂ . Chemistry of Materials, 2016, 28, 2308-2314. | 6.7 | 37 |
| 93 | Anomalous Broadband Spectrum Photodetection in 2D Rhenium Disulfide Transistor. Advanced Optical Materials, 2019, 7, 1901115. | 7.3 | 37 |
| 94 | Electron tunneling at the molecularly thin 2D perovskite and graphene van der Waals interface. Nature Communications, 2020, 11, 5483. | 12.8 | 35 |
| 95 | Flight path of electrospun polystyrene solutions: Effects of molecular weight and concentration. Materials Letters, 2007, 61, 1451-1455. | 2.6 | 34 |
| 96 | Controlled Aqueous Synthesis of 2D Hybrid Perovskites with Bright Room-Temperature Long-Lived Luminescence. Journal of Physical Chemistry Letters, 2019, 10, 2869-2873. | 4.6 | 34 |
| 97 | Wet chemical thinning of molybdenum disulfide down to its monolayer. APL Materials, 2014, 2, . | 5.1 | 31 |
| 98 | Ultrafast charge transfer dynamics pathways in two-dimensional MoS ₂ –graphene heterostructures: a core-hole clock approach. Physical Chemistry Chemical Physics, 2017, 19, 29954-29962. | 2.8 | 31 |
| 99 | Effects Of Structural Phase Transition On Thermoelectric Performance in Lithium-Intercalated Molybdenum Disulfide (Li _{<i>x</i>} MoS ₂). ACS Applied Materials & Interfaces, 2019, 11, 12184-12189. | 8.0 | 31 |
| 100 | Excitonic Energy Transfer in Heterostructures of Quasi-2D Perovskite and Monolayer WS ₂ . ACS Nano, 2020, 14, 11482-11489. | 14.6 | 31 |
| 101 | Significantly enhanced optoelectronic performance of tungsten diselenide phototransistor via surface functionalization. Nano Research, 2017, 10, 1282-1291. | 10.4 | 30 |
| 102 | Emergence of photoluminescence on bulk MoS2 by laser thinning and gold particle decoration. Nano Research, 2018, 11, 4574-4586. | 10.4 | 30 |
| 103 | Graphene Patchwork. ACS Nano, 2011, 5, 4265-4268. | 14.6 | 28 |
| 104 | Hexagonal Boron Nitride Crystal Growth from Iron, a Single Component Flux. ACS Nano, 2021, 15, 7032-7039. | 14.6 | 26 |
| 105 | Observation of the Outâ€ofâ€Plane Polarized Spin Current from CVD Grown WTe ₂ . Advanced Quantum Technologies, 2021, 4, 2100038. | 3.9 | 23 |
| 106 | Sub-Picosecond Carrier Dynamics Induced by Efficient Charge Transfer in MoTe ₂ /WTe ₂ van der Waals Heterostructures. ACS Nano, 2019, 13, 9587-9594. | 14.6 | 22 |
| 107 | Domain Engineering in ReS ₂ by Coupling Strain during Electrochemical Exfoliation. Advanced Functional Materials, 2020, 30, 2003057. | 14.9 | 22 |
| 108 | Measuring Valley Polarization in Two-Dimensional Materials with Second-Harmonic Spectroscopy. ACS Photonics, 2020, 7, 925-931. | 6.6 | 22 |

| # | Article | IF | CITATIONS |
|-----|--|------|-----------|
| 109 | Data-driven discovery of high performance layered van der Waals piezoelectric NbOI2. Nature Communications, 2022, 13, 1884. | 12.8 | 22 |
| 110 | Strong Optical Absorption and Photocarrier Relaxation in 2-D Semiconductors. IEEE Journal of Quantum Electronics, 2015, 51, 1-6. | 1.9 | 21 |
| 111 | Suppressed Out-of-Plane Polarizability of Free Excitons in Monolayer WSe ₂ . ACS Nano, 2019, 13, 3218-3224. | 14.6 | 21 |
| 112 | Hexagonal Boron Nitride Single Crystal Growth from Solution with a Temperature Gradient. Chemistry of Materials, 2020, 32, 5066-5072. | 6.7 | 21 |
| 113 | Impurity-Induced Emission in Re-Doped WS ₂ Monolayers. Nano Letters, 2021, 21, 5293-5300. | 9.1 | 21 |
| 114 | Luminescent Properties of a Waterâ€Soluble Conjugated Polymer Incorporating Grapheneâ€Oxide Quantum Dots. ChemPhysChem, 2015, 16, 1258-1262. | 2.1 | 20 |
| 115 | Polarity Tunable Trionic Electroluminescence in Monolayer WSe ₂ . Nano Letters, 2019, 19, 7470-7475. | 9.1 | 20 |
| 116 | Enhancing charge-density-wave order in 1T-TiSe2 nanosheet by encapsulation with hexagonal boron nitride. Applied Physics Letters, 2016, 109, 141902. | 3.3 | 19 |
| 117 | Quantum Transport Detected by Strong Proximity Interaction at a Graphene–WS2 van der Waals Interface. Nano Letters, 2015, 15, 5682-5688. | 9.1 | 18 |
| 118 | Interlayer screening effects in WS ₂ /WSe ₂ van der Waals hetero-bilayer. 2D Materials, 2018, 5, 041003. | 4.4 | 18 |
| 119 | Harnessing Exciton–Exciton Annihilation in Two-Dimensional Semiconductors. Nano Letters, 2020, 20, 1647-1653. | 9.1 | 18 |
| 120 | Modulating Charge Density Wave Order in a 1T-TaS ₂ /Black Phosphorus Heterostructure. Nano Letters, 2019, 19, 2840-2849. | 9.1 | 17 |
| 121 | Microstructure and Elastic Constants of Transition Metal Dichalcogenide Monolayers from Friction and Shear Force Microscopy. Advanced Materials, 2018, 30, e1803748. | 21.0 | 16 |
| 122 | Layered Hybrid Perovskites for Highly Efficient Threeâ€Photon Absorbers: Theory and Experimental Observation. Advanced Science, 2019, 6, 1801626. | 11.2 | 15 |
| 123 | Synthesis of Twoâ€Dimensional Perovskite by Inverse Temperature Crystallization and Studies of Exciton States by Twoâ€Photon Excitation Spectroscopy. Advanced Functional Materials, 2020, 30, 2002661. | 14.9 | 15 |
| 124 | Electroâ€Optic Upconversion in van der Waals Heterostructures via Nonequilibrium Photocarrier Tunneling. Advanced Materials, 2020, 32, e2001543. | 21.0 | 14 |
| 125 | In-Plane Anisotropic Nonlinear Optical Properties of Two-Dimensional Organic–Inorganic Hybrid Perovskite. Journal of Physical Chemistry Letters, 2021, 12, 7010-7018. | 4.6 | 14 |
| 126 | Valenceâ€band electronic structure evolution of graphene oxide upon thermal annealing for optoelectronics. Physica Status Solidi (A) Applications and Materials Science, 2016, 213, 2380-2386. | 1.8 | 13 |

| # | Article | IF | CITATIONS |
|-----|--|------|-----------|
| 127 | Observation of wrinkle induced potential drops in biased chemically derived graphene thin film networks. Carbon, 2013, 64, 35-44. | 10.3 | 11 |
| 128 | Elastomeric Waveguide on-Chip Coupling of an Encapsulated MoS2 Monolayer. ACS Photonics, 2019, 6, 595-599. | 6.6 | 11 |
| 129 | Bundling dynamics of single walled carbon nanotubes in aqueous suspensions. Journal of Applied Physics, 2008, 103, 093118. | 2.5 | 9 |
| 130 | Exciton Polarization and Renormalization Effect for Optical Modulation in Monolayer Semiconductors. ACS Nano, 2019, 13, 9218-9226. | 14.6 | 9 |
| 131 | Disorder-driven two-dimensional quantum phase transitions in Li <i> _x </i> MoS ₂ . 2D Materials, 2020, 7, 035013. | 4.4 | 7 |
| 132 | Tuning photoresponse of graphene-black phosphorus heterostructure by electrostatic gating and photo-induced doping. Chinese Chemical Letters, 2022, 33, 368-373. | 9.0 | 5 |
| 133 | Inâ€Plane Fieldâ€Driven Excitonic Electroâ€Optic Modulation in Monolayer Semiconductor. Advanced Optical Materials, 2022, 10, . | 7.3 | 4 |
| 134 | Mode enter Placement of Monolayer WS 2 in a Photonic Polymer Waveguide. Advanced Optical Materials, 0, , 2101684. | 7.3 | 3 |
| 135 | Dynamic Tuning of Moiré Superlattice Morphology by Laser Modification. ACS Nano, 2022, 16, 8172-8180. | 14.6 | 3 |
| 136 | Chalcogenide Nanosheets: Optical Signatures of Many-Body Effects and Electronic Band Structure. Nanostructure Science and Technology, 2017, , 133-162. | 0.1 | 2 |
| 137 | Phase coherent transport in bilayer and trilayer MoS2. Physical Review B, 2019, 100, . | 3.2 | 2 |
| 138 | Phase Matching via Plasmonic Modal Dispersion for Third Harmonic Generation. Advanced Science, 2022, 9, . | 11.2 | 2 |
| 139 | Feature issue introduction: two-dimensional materials for photonics and optoelectronics. Optical Materials Express, 2016, 6, 2458. | 3.0 | 1 |
| 140 | In-Situ Raman Spectroscopy of Graphene Defects in Reducing Atmospheres at High Temperature. , 2010, , | | 0 |
| 141 | Charge Transport and Exciton Dynamics in 2D Semiconductors. , 2014, , . | | 0 |
| 142 | Coupling 2D Materials to an Elastomer Waveguide. , 2019, , . | | 0 |
| 143 | TMDâ€Based Phototransistors: Anomalous Broadband Spectrum Photodetection in 2D Rhenium Disulfide Transistor (Advanced Optical Materials 23/2019). Advanced Optical Materials, 2019, 7, 1970088. | 7.3 | 0 |